[CANCER RESEARCH 63, 8037–8050, November 15, 2003]

Signaling Pathways of Apoptosis Activated by Aromatase Inhibitors and Antiestrogens

Apinya Thiantanawat, Brian J. Long, and Angela M. Brodie

Department of Pharmacology and Experimental Therapeutics, University of Maryland School of Medicine, Baltimore, Maryland

ABSTRACT

Aromatase inhibitors have recently been reported to be more effective than the antiestrogen tamoxifen (Tam) in treating breast cancer. Here, we studied the mechanisms and signaling pathways of cell growth, cell cycle progression, and apoptosis induced by three aromatase inhibitors: letrozole (Let), anastrozole, and 4-hydroxyandrostenedione in comparison with estrogen withdrawal (E2W) and antiestrogens Tam and faslodex. Estrogen-dependent human breast cancer cells stably transfected with aromatase (MCF-7Ca) were used. All treatments induced growth suppression and cell cycle arrest at the G_0-G_1 phase that was associated with up-regulation of p53 and p21 protein and mRNA levels and down-regulation of *cyclin D1* and *c-myc* mRNA. The apoptotic index was increased 4–7 fold, Bcl-2 protein expression decreased, Bax increased, and caspase-9, caspase-6, and caspase-7 were activated but not caspase-3 and caspase-8. Let and E2W caused regression of tumors of MCF-7Ca cells grown in nude mice and increased the number of cells undergoing apoptosis. In contrast, Tam and faslodex did not induce tumor regression and a lower number of apoptotic cells was detected. Cleavage of poly(ADP-ribose) polymerase was detected. Treatment with Let, Tam, or E2W resulted in a dose- and time-dependent increase in active caspase-7 and up-regulation of p53 and p21 protein. Although the mechanisms involved appeared to be similar for antiestrogens and aromatase inhibitors, the most significant effects occurred with Let, which were significantly greater than with E2W and consistent with marked effects of Let on tumor and cell growth.

INTRODUCTION

For many years, research in the field of endocrine-mediated breast cancer has focused on the proliferative effects of estrogen. However, recent work has also demonstrated a role for this steroid hormone on the suppression of apoptosis (1, 2). Apoptosis is the highly orchestrated process of cell death. Apoptosis can be initiated by a wide variety of stimuli, including developmental signals, cellular stress, and disruption of cell cycle (3). However, the execution of apoptosis is remarkably uniform, involving characteristic morphological and biochemical changes (4). A number of the key factors involved in the regulation, coordination, and execution of apoptosis have been identified. Among them, the Bcl-2 family of proteins is a critical regulator of apoptosis, acting to either inhibit or promote cell death. In addition, most of the morphological changes that occur during apoptosis are caused by a set of cysteine proteases named caspases (5, 6).

Unlike most types of cancer, breast cancer is known to be under hormonal control. Estrogen has been reported to stimulate the growth of breast cancer expressing functional ERs[1] by affecting the cell cycle machinery (7, 8) and by inducing specific growth factors and their receptors (9). In addition to inducing breast cancer cell proliferation, estrogen prevents the induction of apoptosis, at least in part, by altering the expression of the Bcl-2 family of proteins. Treatment of MCF-7 breast cancer cells with E_2 results in a decrease in proapoptosis Bax (2) and an increase in antiapoptosis Bcl-2 mRNA and protein (1). It has been reported that E_2 deprivation or antiestrogen treatment induces apoptotic cell death in MCF-7 tumors (10, 11). Recent studies have shown that the induction of apoptosis and inhibition of proliferation associated with E_2 deprivation of MCF-7 tumors was associated with increased expression of ER, p27 protein levels, p21 protein levels, and a decrease in Bcl-2, cyclin D1, and Rb protein expression (12, 13).

Hormonal therapies have an important role in treating ER-positive breast cancer patients. Currently, two pharmacological strategies are used to ameliorate the proliferative effects of estrogens. One is the inhibition of estrogen action using antiestrogens that interact with the ER. The other is the inhibition of estrogen synthesis by inhibitors of aromatase (14). The antiestrogen Tam has been shown to produce a significantly better response rate than chemotherapy in postmenopausal patients with ER-positive breast cancer. However, resistance to Tam inevitably develops and is mediated, in part, by its partial agonist properties. Aromatase inhibitors are a new group of drugs that are clinically useful in advanced breast cancer and Tam-resistant patients. These compounds block the synthesis of estrogens and do not have estrogenic activity (15). Compared with Tam, treatment with the aromatase inhibitor Let has been shown to be superior to Tam in our preclinical model (16) and recently in breast cancer patients also (17). Let treatment causes regression in MCF-7 human breast cancer cells transfected with the aromatase gene (MCF-7Ca) and grown as tumors in nude mice. This suggested that the net decrease in cell number is being induced by apoptosis. To date, there have been no studies on the molecular mechanisms of apoptosis induced by aromatase inhibitor.

In this study, we have investigated the effects of the aromatase inhibitors: Let, Anas, and 4-OHA compared with the antiestrogens Tam and Fas and E2W condition on cell cycle progression and induction of apoptosis. The estrogen-dependent human breast cancer cell line (MCF-7) stably transfected with the human aromatase gene (Ref. 18; MCF-7Ca) was used to study the molecular pharmacology associated with treatment with aromatase inhibitors. We have identified the molecular mechanisms and signaling pathways activated during induction of apoptosis by focusing on the involvement of antiapoptotic proteins, proapoptotic proteins, and caspases. In addition, we demonstrated the *in vivo* effects of Let compared with Tam, Fas, and E2W on inducing apoptosis of MCF-7Ca grown as tumors in nude mice. Finally, we have correlated protein expression with mRNA expression to additionally characterize the molecular mechanisms associated with treating MCF-7Ca breast tumor xenografts with aromatase inhibitor and antiestrogen.

Received 5/23/03; revised 8/12/03; accepted 9/2/03.

Grant support: Supported by National Cancer Institute, NIH Grant CA-62483 (to A. M. B.). A. T. was supported in part by the Predoctoral Traineeship Award in Breast Cancer Research Program from the United States Army Medical Research Materiel Command under DAMD17-00-1-0325.

The costs of publication of this article were defrayed in part by the payment of page charges. This article must therefore be hereby marked *advertisement* in accordance with 18 U.S.C. Section 1734 solely to indicate this fact.

Requests for reprints: Angela M. Brodie, Department of Pharmacology and Experimental Therapeutics, School of Medicine, University of Maryland, 685 West Baltimore Street, Health Science Facility, Room 580G, Baltimore, MD 21201. Phone: (410) 706-3137; Fax: (410) 706-0032; E-mail: abrodie@umaryland.edu.

[1] The abbreviations used are: ER, estrogen receptor; E_2, 17β-estradiol; DPBS, Dulbecco's phosphate-buffered saline; P/S, penicillin/streptomycin; G418, Geneticin; FBS, fetal bovine serum; AD, androstenedione; Let, letrozole; Anas, anastrozole; 4-OHA, 4-hydroxyandrostenedione; 4-OHTam, 4-hydroxy tamoxifen; Tam; tamoxifen; Fas, faslodex; E2W, estrogen withdrawal; PI, propidium iodide; TUNEL, terminal deoxynucleotidyl transferase-mediated nick end labeling; RPA, ribonuclease protection assay; PARP, poly(ADP-ribose) polymerase; PCNA; proliferating cell nuclear antigen; Cdk, cyclin-dependent kinase.

MATERIALS AND METHODS

Materials

DMEM, P/S, trypsin/EDTA solution, DPBS, and G418 were purchased from Life Technologies, Inc. (Grand Island, NY). Phenol red-free improved minimum essential medium (without partial remission) and phenol red-free trypsin/EDTA were obtained from Biofluids, Inc. (Rockville, MD). FBS and dextran-coated charcoal-treated serum were from Hyclone (Logan, UT). E2, AD, 4-OHTam, Tam, PI, RNase (DNase free), 10% neutral-buffered formalin, poly-L-lysine, RNA later, and paraformaldehyde were purchased from Sigma-Aldrich Chemical Company (St. Louis, MO). Let was generously provides by Dr. Dean Evans (Novartis Pharmaceuticals, Basel, Switzerland). Anas and Fas were kindly supplied by Dr. Alan Wakeling (Astra Zeneca Pharmaceuticals, Macclesfield, United Kingdom). 4-OHA was synthesized in our laboratory (15).

Cell Line

The MCF-7 human breast cancer cell line stably transfected with the human aromatase gene, designated MCF-7Ca (18), were kindly provided by Dr. Shiuan Chen (City of Hope, Duarte, CA). MCF-7Ca cells were maintained in a standard medium of DMEM supplemented with 5% FBS, 1% P/S, and 700 μg/ml G418. Cells were cultured at 37°C in a humidified incubator with 5% CO_2 and 95% air.

Cell Synchronization

MCF-7Ca cells (1.5×10^6 cells) were plated into a T-75 flask and were cultured in standard medium for 4 days. Then to circumvent interference from the steroids present in FBS and the estrogenic effect of phenol red, cells were switched to E_2-free medium, which consisted of improved MEM without phenol red with 5% dextran-coated charcoal-treated serum, 1% P/S, and 700 μg/ml G418 4 days before the start of the experiments (day -4). At day -1, cells were harvested by trypsinization. Cells were synchronized at G_1 phase of cell cycle by this procedure before each experiment.

Cell Growth Assay

At day -1, flasks of 80% confluent synchronized MCF-7 Ca cells were harvested by trypsinization. Cells were seeded in triplicate into 24-well plates at 1×10^4 cells/well and were allowed to attach overnight. On day 0 of the experiment, the medium was replaced with fresh medium containing the aromatase substrate, AD at a concentration of 25 nM. The three aromatase inhibitors, Let, Anas, and 4-OHA at concentrations of 1–1000 nM, and the two antiestrogens, 4-OHTam and Fas at a concentration of 1000 nM, were added to medium to test their effects on cell growth. Cells cultured without AD designated E2W were treated with ethanol vehicle. The medium and drugs were refreshed every 3 days. On day 8 of treatment, the cells were harvested, and total cell number was determined using a Coulter Counter.

Cell Cycle Analysis

On day -1 of the experiments, synchronized MCF-7 Ca cells were plated into T-75 flasks at 5×10^5 cells and allowed to adhere overnight. On day 0, the cells were treated with 1 μM Let, Anas, 4-OHA, 4-OHTam, or Fas in the presence of AD (25 nM). The medium containing the appropriate treatments was changed on day 3 and day 6. Cells were harvested on days 3, 6, and 8 of treatment, washed twice with DPBS, and were fixed with 100% cold ethanol. Cells were stained with PI solution (50 μg/ml PI in DPBS, 0.5 μg/ml RNase-DNase free), and the fluorescence of individual nuclei (10,000 events) was analyzed by flow cytometry (Becton Dickinson FACScan). The percentage of cells in the G_0-G_1, S, and the G_2-M phases of the cell cycle was determined using ModFitLT V3.1 (Verity Software House, San Jose, CA).

Caspase Activity Assays

Caspase activation was determined using a caspase-3 cellular activity assay kit, a caspase-6 colorimetric assay kit, and a caspase-8 assay kit from Calbiochem-Novabiochem (San Diego, CA) as recommended by the manufacturer's instructions. Briefly, 100 μg of whole cell lysates were used for the assays. The volume of cell lysates was adjusted to 50 μl with lysis buffer, and 50 μl of 2× reaction buffer were added to each sample. Five μl of 4 mM substrate DEVD-*p*NA (caspase-3), VEID-*p*NA (caspase-6), or Ac-IETD-*p*NA (caspase-8) were added, and the samples were incubated at 37°C for 1 h. Absorbance of the samples was read at 405 nm in a microtiter plate reader. The changes in activity were determined as a percentage of the vehicle-treated cells.

Animals

Ovariectomized female BALB/c athymic nude mice 4–6 weeks of age were obtained from National Cancer Institute (Frederick, MD). The animals were housed in a pathogen-free environment under controlled conditions of light and humidity and received food and water *ad libitum*. All animal studies were performed according to the guidelines and approval of the Animal Care Committee of the University of Maryland School of Medicine.

MCF-7Ca Xenograft Tumor Growth in Female Athymic Nude Mice

Subconfluent MCF-7Ca cells cultured in DMEM with 5% FBS, 1% P/S, and 700 μg/ml G418 were harvested by scraping. Cells were collected by centrifugation, washed in DPBS and resuspended in Matrigel (10 mg/ml) at 2.5×10^7 cells/ml. Each ovariectomized mouse received s.c. injections at two sites in each flank with 0.1 ml of the cell suspension (2.5×10^6 cells/site). AD (100 μg/day, s.c.) was injected 1 day after cell inoculation and, unless noted, was continued for the duration of the experiment. Tumor volumes were measured weekly with calipers and were calculated using the formula $4/3\pi \times r_1^2 \times r_2$ ($r_1 < r_2$). Treatments began when the tumor volumes reached 300 mm^3. Animals were grouped so that total tumor volume of each group was approximately the same. Animals then received s.c. injections of Let (10 or 100 μg/day), Tam (100 μg/day), or (Fas 1 mg/day) in addition to the AD supplement. Control mice received s.c. injections of AD only. E2W mice received s.c. injections of vehicle (0.3% hydroxypropyl cellulose, 0.1 ml/day) without AD supplement. Animals were treated for the indicated time periods, after which, they were sacrificed by decapitation, and the blood was collected. Tumors and uteri were excised, cleaned, and weighed. Harvested tumors were placed on ice and rapidly fixed in 10% neutral-buffered formalin (Sigma-Aldrich Chemical Co.) overnight before being embedded in paraffin for immunohistochemistry or stored in RNAlater solution at −80°C for protein and gene expression analysis.

Detection of Apoptosis

***In Vitro* Assay.** Synchronized MCF-7Ca cells were treated with Let, Anas, 4-OHA, or Fas at concentrations 100 and 1000 nM in the presence of AD (25 nM). E2W cells were cultured in steroid-free medium in the absence of AD. On day 8 of treatment, adherent cells were harvested by trypsinization and combined with cells floating in the media. Cells were washed with ice-cold DPBS, and 1×10^6 cells were suspended in 0.5 ml of DPBS. The cell suspension was fixed by adding 5 ml of 1% (w/v) paraformaldehyde in DPBS and incubated on ice for 15 min. Cells were washed twice with ice-cold DPBS before being fixed overnight at −20°C in 70% (v/v) ethanol. Apoptosis was determined by the TUNEL method using the APO-Br dUTP kit (Phoenix Flow Systems, Inc., San Diego, CA) according to the manufacturer's directions. Apoptotic cells were detected by flow cytometry analysis. Data were analyzed by using CELLQuest-BrdUrd software from Phoenix Flow Systems, Inc.

***In Situ* TUNEL Assay.** Paraffin fixed tissue sections 4-μm thick were spread on poly-L-lysine coated slides. The slides were pretreated with proteinase K (20 μg/ml, 15 min) before TUNEL staining using ApopTag Plus Peroxidase *In Situ* Apoptosis Detection kit for immunoperoxidase staining (Intergen, Purchase, NY) according to the manufacturer's instructions.

Preparation of Total Cell Lysates

Adherent and floating cells were harvested after 1, 2, 3, and 4 days of treatment. The floating cells were collected by centrifugation at $500 \times g$ (4°C) for 20 min, and the cells that remained attached to the culture flask were detached by scraping. Both the floating and attached cells were mixed together, centrifuged, and washed in 20 ml of ice-cold DPBS. The cell pellet was resuspended in chilled cell lysis buffer [0.1 M Tris HCl, 0.5% Triton X-100, protease inhibitors mixture (Complete TM; Boehringer, Indianapolis, IN)] and sonicated for 20 s. The homogenates were transferred to new Eppendorf tubes

and were incubated on ice for 30 min. The homogenates were spun at 10,000 × *g* for 30 min, and supernatants were separated and stored at −80°C.

Tumors were thawed on ice, washed, and homogenized in ice-cold T-PER Tissue Protein Extraction Reagent (Pierce, Rockford, IL) plus protease inhibitors mixture. The homogenates were centrifuged at 5000 × *g* at 4°C for 30 min. Supernatants were stored at −80°C. Protein concentrations were determined using a Bio-Rad kit (Bio-Rad, Hercules, CA).

Gel Electrophoresis and Western Blotting

Equal amounts of total protein (50–100 μg) were subjected to SDS-PAGE (60 V, 3 h), using the mini-Protean3 electrophoresis module assembly (Bio-Rad) and transferred (90 V, 1 h) to nitrocellulose membranes (Hybond ECL; Amersham, Buckinghamshire, UK). Immunodetections were performed using mouse monoclonal antibodies against human Bcl-2, human caspase-9, actin, rabbit polyclonal antibodies against human Bax (Oncogene Research Products, Boston, MA), rabbit polyclonal antibodies against human caspase-7 (Cell Signaling Technology, Beverly, MA), mouse monoclonal antibodies against human p21, mouse monoclonal antibodies against human p53 (Upstate Biotechnology, Lake Placid, NY), or purified mouse antihuman PARP monoclonal antibody (BD PharMingen, San Diego, CA). Immunoreactive bands were visualized using the enhanced chemiluminescence detection reagents (Amersham Corp., Arlington Heights, IL) according to the manufacturer's instructions and quantitated by densitometry using Bio-Rad software (Quantity One).

RNA Isolation and RPA

Total RNA, free from DNA, was isolated from MCF-7Ca tumors using the Trizol reagent (Invitrogen, Carlsbad, CA). The purity and integrity of the RNA isolated were determined by UV absorbance spectrophotometer and by agarose gel electrophoresis, respectively.

The RiboQuant Multiprobe protection assay system (BD PharMingen) was used for simultaneous detection and quantification of multiple mRNA species. We used customized templates (Custom human template set; BD PharMingen) to detect levels of *bcl-2*, *bax*, *PARP*, *caspase-3*, *caspase-6*, *caspase-7*, *caspase-8*, *caspase-9*, *p53*, *p21*, *cyclin D1*, *PCNA*, and *c-myc* mRNAs. The template also included two housekeeping genes, *L32* and *GADPH*, as internal standards. The assays were preformed as described in the manufacturer's protocol. Briefly, ^{32}P-labled antisense RNA was transcribed *in vitro* using T7 RNA polymerase (PharMingen) and [α-^{32}P]UTP (Amersham Life Science, Piscataway, NJ). Twenty μg of total RNA were hybridized with excess of ^{32}P-labeled probes at 56°C for 16 h. Single-stranded and unhybridized excess mRNA was digested by RNase-DNase free (PharMingen). The protected hybridized double-stranded RNA was precipitated, dried, and resuspended in 5 μl of 1× loading buffer (PharMingen). Samples were separated by electrophoresis in a standard sequencing gel of 5% polyacrylamide-8 M urea gel, 0.5% Tris-boric acid-EDTA at 50 W. The gel was dried on blotting paper for 1 h at 80°C. The dried gel was placed on BioMax MR film (Eastman Kodak Company, Rochester, NY) and was exposed at −70°C. For comparative analysis, the mRNA levels of each gene were quantitated as a percentage of the ribosomal protein *L32* mRNA levels.

Statistical Analysis

The statistical differences were analyzed using the Student's *t* test on SigmaPlot 2000. All statistical tests were two sided, and differences were considered to be statistically significant when $P < 0.05$.

RESULTS

Aromatase Inhibitor and Antiestrogen Inhibit Growth of MCF-7Ca Cells in Culture. To address the direct effect of aromatase inhibitors on the proliferation of MCF-7Ca cells in culture, cells were cultured in E_2-free medium 4 days before the experiment. The aromatase substrate, AD, was then added as the source of E_2 synthesis. The optimum concentration of AD that induced cell proliferation to a level comparable with E_2 (1 nM) in cells grown in normal medium after 8 days of treatment was 25 nM (Fig. 1*A*). This concentration of AD was added on day 0 of all future experiments of MCF-7Ca cells in culture. The three aromatase inhibitors Let, Anas, and 4-OHA at concentrations 1–1000 nM dramatically reduced AD-induced cell proliferation in a dose-dependent manner (Fig. 1*B*). The antiproliferative effects of aromatase inhibitors were comparable with that induced by E2W. At the same concentration (1000 nM), all three aromatase inhibitors showed greater growth inhibitory effects than antiestrogens 4-OHTam and Fas ($P < 0.005$ for 4-OHTam and $P < 0.05$ for Fas *versus* the aromatase inhibitors).

Aromatase Inhibitors and Antiestrogens Induce Disruption of Cell Cycle Progression and Activation of Apoptosis. To investigate the causes of the antiproliferative effects of aromatase inhibitors and antiestrogens, cells were stained with PI, and cell cycle analysis was performed by flow cytometry. The cell cycle profile of MCF-7Ca cells treated with aromatase inhibitors, antiestrogens, and E2W were similar as each treatment increased in the percentage of cells in the G_0-G_1 phase of the cell cycle and reduced the fraction of cells in the S and G_2-M phases (Table 1). Among all of the treatments, Let caused the greatest accumulation of cells (83.42%) in the G_0-G_1 phase. This compared with 49.70% in the control. In response to treatment with Let, there was also a significant decrease ($P < 0.005$) in the number of cells in S phase (10.56%) and G_2-M phase (6.01%). This compared with 35.22 and 15.07%, respectively, in the control-treated cells. These effects of aromatase inhibitors and antiestrogens on cell cycle progression were detected starting on day 3 of treatment (Table 1) and were continued to day 6 and day 8 (data not shown).

In addition to inhibiting cell cycle progression, we also examined whether treatment with aromatase inhibitors and antiestrogens was reducing cell number by inducing cell death. PI staining for DNA content showed an increase in the percentage of cells in the sub-G_1 phase (data not shown), which raised the possibility that cells were undergoing apoptosis. To investigate this possibility, TUNEL assays, which detect DNA fragmentation (a characteristic of apoptosis), were performed using flow cytometry analysis. After 8 days of treatment, Let (100 and 1000 nM) induced apoptosis by 14.38 and 13.51%, respectively, compared with 1.82% of the control cells (Fig. 2). Treatment with Anas (1000 nM) induced apoptosis in 13.07% of cells and 4-OHA (100 and 1000 nM) in 9.46 and 10.77% of cells, respectively. The induction of apoptosis by Let and Anas was comparable with that induced by E2W. Interestingly, the level of apoptosis induced by pure antiestrogen Fas (9.44%) was lower than that induced by Let and Anas.

Taken together, these results indicated that the antiproliferative effects of aromatase inhibitors and antiestrogens on MCF-7Ca cells are mediated by disrupting cell cycle progression by causing growth arrest at the G_1 phase of cell cycle and by inducing cell death by apoptosis.

Apoptosis Induced by Let, 4-OHTam, Fas, and E2W Involves Down-Regulation of Bcl-2 and Up-Regulation of Bax Protein Expression. After observing induction of apoptosis by aromatase inhibitors and antiestrogens, we set out to examine the mechanisms involved. Because Let was the most effective of the three inhibitors, we tested this compound in comparison to 4-OHTam, Fas, and E2W.

We first investigated the effect of Let, 4-OHTam, Fas, and E2W on the expression of Bcl-2 protein. All treatments induced a decrease in the level of Bcl-2 protein when compared with the control. This reduction was detectable on day 1 of treatment, and there was an additional decrease on day 2 of treatment (Fig. 3*A*). Let induced down-regulation of Bcl-2 protein in dose- and time-dependent manner. Quantitative analysis showed a reduction to 0.46, 0.27, and 0.25-fold of control by Let concentrations of 10, 100, and 1000 nM, respectively, on day 2 of treatment. Treatment with the antiestrogens 4-OHTam and Fas decreased Bcl-2 protein expression more than the aromatase inhibitors to 0.17- and 0.08-fold when compared with

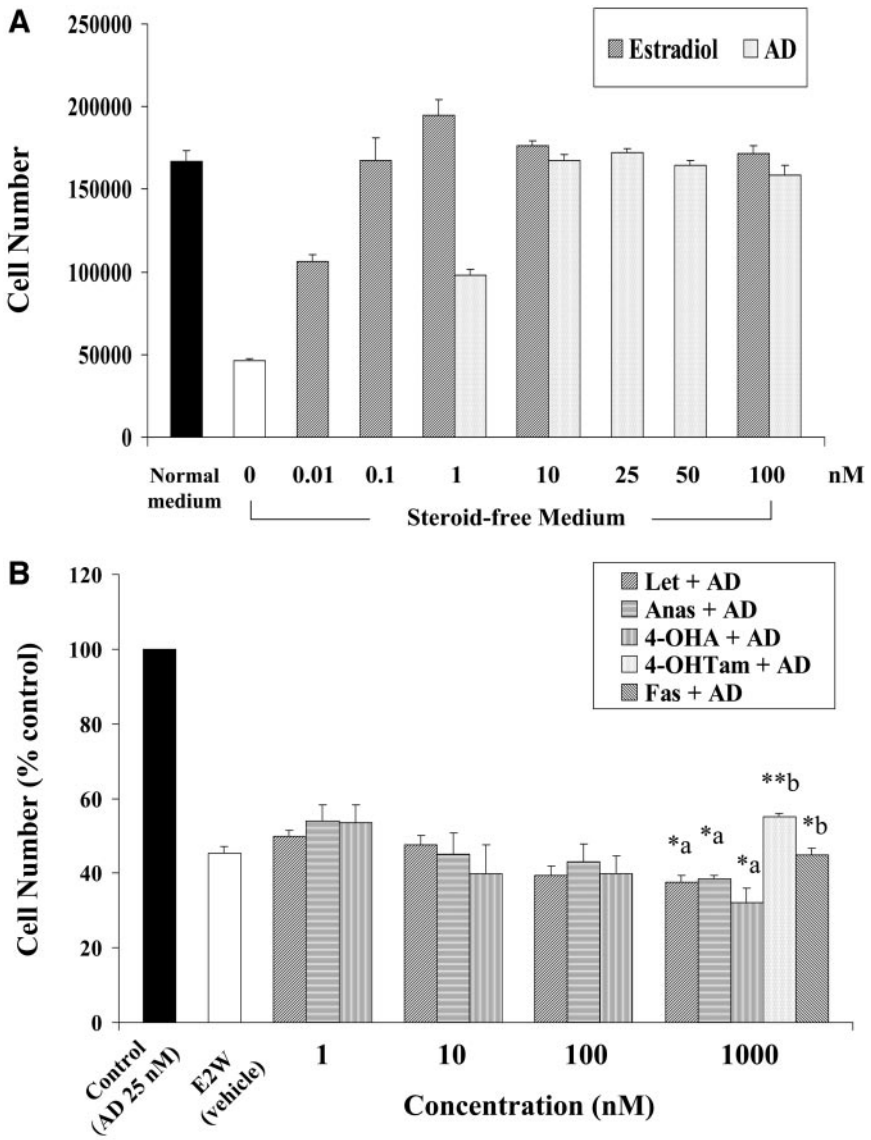

Fig. 1. *A*, the effect of E2 and AD on the growth of MCF-7Ca human breast cancer cells *in vitro*. *B*, *in vitro* antiproliferative effects of Let, Anas, 4-OHA, 4-OHTam, and Fas in the presence of 25 nM AD and E2W (vehicle without AD) on MCF-7Ca human breast cancer cells. MCF-7Ca cells were cultured in steroid-free medium without phenol red for 3 days before plating. Triplicate wells were then treated with the indicated concentrations of E_2, AD, aromatase inhibitors, or antiestrogens for 8 days, and the media were refreshed every 3 days. Cell numbers are expressed as (*A*) actual cell number in each well and (*B*) a percentage of the mean number of cells in the control (AD) wells. The results showed the mean and SE from triplicate experiments. *a*, statistically different *versus* E2W; *b*, statistically different *versus* aromatase inhibitors in equivalent concentrations (*, $P < 0.05$; **, $P < 0.005$).

control. On day 2, E2W decreased the Bcl-2 levels to a less extent than all other treatments to 0.46-fold of control. On day 3 and day 4, the reduction in Bcl-2 protein levels after treatment was less than the levels on day 2 (data not shown).

We next examined the effects of Let, 4-OHTam, Fas, and E2W on expression of the proapoptotic protein Bax. MCF-7Ca cells showed increased expression of Bax in response to all treatments when compared with control. Obvious quantitative changes were seen on day 1 with the peak on day 2 of treatment (Fig. 3*B*). These increases were maintained through day 3 and day 4 of treatment (data not shown). On day 2, 4-OHTam and Fas increased Bax protein levels to 2.9- and 2.5-fold of control similar to the increase by E2W of 2.7-fold. Let (10, 100, and 1000 nM) up-regulated Bax protein expression to a greater extent with increase of 5.2-, 3.6-, and 4.0-fold, respectively.

Table 1 *Effects of aromatase inhibitors and antiestrogens treatment on cell cycle distribution*[a]

Treatments[b]	Cell cycle distribution (percentage of cells)		
	G_0-G_1	S	G_2-M
Control [AD (25 nM)]	49.70 ± 2.93	35.22 ± 4.05	15.07 ± 2.20
Let (100 nM) + AD (25 nM)	83.42 ± 1.47[c]	10.56 ± 1.32[c]	6.01 ± 2.79[d]
Anas (100 nM) + AD (25 nM)	64.17 ± 2.67[d]	30.37 ± 0.26	4.50 ± 1.68[b]
4-OHA (100 nM) + AD (25 nM)	67.11 ± 1.77[e]	24.08 ± 2.12	8.80 ± 3.11
4-OHTam (100 nM) + AD (25 nM)	66.94 ± 9.75	27.13 ± 7.09	5.92 ± 2.69[d]
Fas (100 nM) + AD (25 nM)	70.24 ± 11.20	27.69 ± 10.91	2.08 ± 1.69[e]
E2W (vehicle)	75.97 ± 0.84[c]	19.14 ± 0.84[d]	4.87 ± 0.56[c]

[a] Results (percentage of cells distribute in cell cycle) are expressed as mean ± SE ($n = 3$ independent experiments).
[b] Duration of treatment is 3 days.
[c] Significantly different compared with the corresponding control value ($P < 0.005$).
[d] Significantly different compared with the corresponding control value ($P < 0.05$).
[e] Significantly different compared with the corresponding control value ($P < 0.01$).

Effects of Let, 4-OHTam, and Fas on the Activation of Caspases in MCF-7Ca Cells. The involvement of Bcl-2 and Bax implied that induction of apoptosis by these treatments may be via the mitochondrial pathway. We next examined whether caspase-9, a molecule that plays a major role as an initiator caspase in this pathway, was activated. To address this question, we used an antibody to caspase-9 that can detect both the pro- and active forms of the protein. In comparison to control, Let (100 and 1000 nM) increased expression of the active-form (M_r 35,000) of caspase-9 by 1.2- and 1.5-fold, respectively, after 3 days of treatment. The greatest increase was seen on day 4 of treatment with 1.6-, 2.2-, and 2.0-fold increases by Let concentrations of 10, 100, and 1000 nM, respectively (Fig. 3*C*). E2W cells showed significantly less increase in expression of the active form by 1.6- and 1.4-fold on day 3 and day 4, respectively. Fas treatment

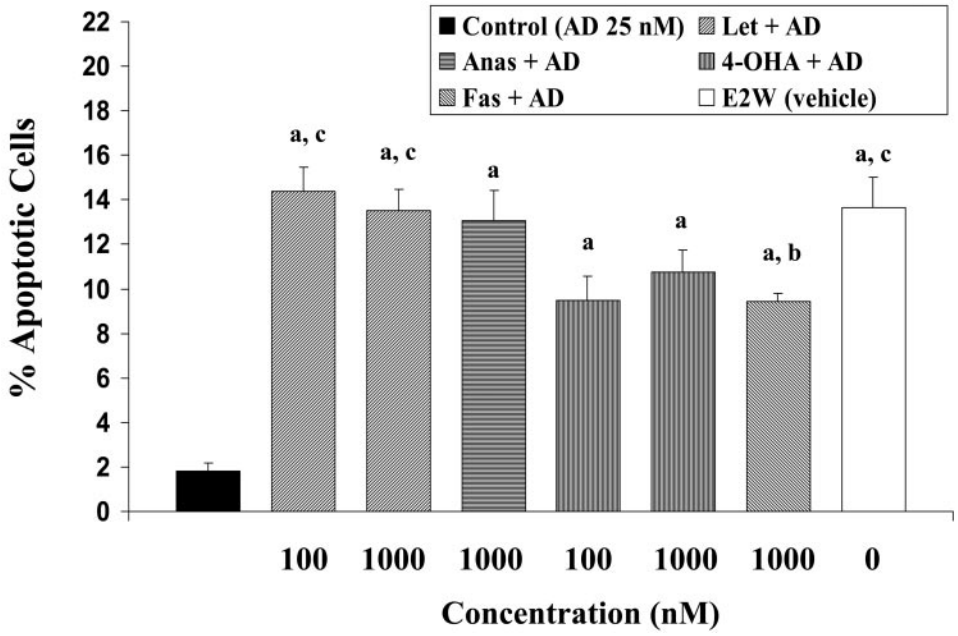

Fig. 2. Induction of apoptosis in MCF-7Ca cells as determined by the TUNEL assay. MCF-7Ca cells were cultured in steroid-free medium for 4 days before cells (1×10^7 cells) were seeded to new T-75 flasks. Cells were cultured in steroid-free medium plus 25 nM AD overnight before new medium was added. Cells were treated with 100 and 1000 nM of the tested drugs (Let, Anas, 4-OHA, or Fas) in the presence of 25 nM AD. Control cells were cultured in steroid-free medium with AD (25 nM), and E2W cells were cultured in the absence of AD. The medium was refreshed every 3 days and on day 8 of treatment, cells were harvested as described in "Materials and Methods." Percentages of apoptotic cells were quantitated from three independent experiments. Data are presented as mean ± SE. *a*, statistically different *versus* control; *b*, statistically different *versus* E2W; *c*, statistically different *versus* Fas ($P < 0.05$).

increased expression of the active-form of caspase-9 to about the same extent as E2W. Interestingly, 4-OHTam had only a modest effect on expression of the active-form of caspase-9, which increased by 1.2- fold.

To identify whether other caspases downstream of caspase-9 were affected, caspase activity assays were performed. Caspase-3 is believed to be the major effector caspase that functions downstream of caspase-9. It has been reported that caspase-3 in MCF-7 cells is nonfunctional (19, 20). Using a caspase-3 substrate (DEVD-*p*NA), no induction of caspase-3 was detected after treatment with Let, 4-OH-Tam, Fas, and E2W in MCF-7Ca cells (data not shown). This suggests the involvement of other effector caspases in apoptosis induced in MCF-7Ca cells after treatments with aromatase inhibitors and antiestrogens.

Another caspase activity assay using a caspase-6-specific substrate (VEID-*p*NA) was performed. No induction in caspase-6 activity was detected on day 1 and day 2 after treatment (data not shown). The activity was slightly increased on day 3 of treatment (Fig. 4). On day 4, the caspase-6 activity in Let-treated cells was increased in the range of 160–190% of control in a concentration-dependent manner. The activity was comparable with that induced by E2W. 4-OHTam and Fas-treatment caused a smaller increase in caspase-6 activity than Let-treatment with activity of 150 and 130% of control, respectively.

We also analyzed whether caspase-8, the initiator caspase in death receptor-mediated pathway, is involved in apoptotic activation in our test system. Examination of caspase-8 activity using caspase-8-specific substrate Ac-IETD-*p*NA revealed no increase in activation of caspase-8 activity (data not shown). Therefore, the apoptotic-signaling pathway activated by aromatase inhibitors and antiestrogens is likely to be mediated via the mitochondrial pathway.

The Effect of Let, Tam, Fas, and E2W on MCF-7Ca Tumors Growth in Female Ovariectomized Nude Mice. After data were obtained from MCF-7Ca grown in culture, we use the MCF-7 Ca tumor xenograft model to examine the effects of therapies on tumor growth *in vivo*. An *in vivo* intratumoral aromatase nude mouse model that simulates, to some extent, postmenopausal, hormone-dependent breast cancer has been developed and established in our laboratory (21). Using this model, the effects on MCF-7Ca tumor growth of Let, Tam, Fas, and E2W compared with control were studied. Daily s.c. injections of AD (100 μg) were sufficient to induce MCF-7Ca cells to form tumors in ovariectomized nude mice. Mean tumor volumes reached 300 mm^3 after 6 weeks of AD administration. As shown in Fig. 5*A*, Let (10 and 100 μg) induced regression in tumor growth. This effect was evident as early as day 3 of treatment, and tumor volumes continued to reduce over the duration of experiment. On day 14 of treatment, Let (10 μg/day) and Let (100 μg/day) had reduced tumor volumes to 54 and 62% of the initial volume, respectively. Tumor volumes in the control animals were increased by 135% on day 14 of treatment. Although the antiestrogens Tam and Fas reduced the rate of tumor growth (105 and 98%, respectively, at day 14) when compared with control, neither treatment caused a regression in tumor volume. In animals receiving only the vehicle, which mimics the estrogen withdrawal conditions, tumor volume also decreased (80% of the initial volume at day 14 of treatment) but to a lesser extent than that observed in the Let-treated groups. On day 14 of treatment, mean tumor volume in Let 10- and 100-μg groups were significantly lower than in E2W group ($P = 0.001$ and 0.016, respectively).

At the indicated time periods of treatment, animals were sacrificed, and the tumors were removed, cleaned, weighed, and stored at −80°C. The uterus was also removed from each animal and weighed. It has been reported that the weight of uterus is correlated with the levels of circulating estradiol in this model (16, 22). The uterine weights of the Let-treated animals were significantly less than those of the control animals (Fig. 5*B*). The reduction in uterine weight by Let treatment was evident as early as day 3 of treatment ($P < 0.001$ *versus* control) and was prolonged through day 14 of treatment ($P < 0.001$ on day 7 and $P < 0.05$ on day 14 *versus* control). Uterine weights in E2W animals were also decreased, but the reduction occurred more slowly than in the Let-treated animals ($P < 0.05$ on day 7 and day 14 *versus* control). Animals treated with Fas also showed a significant decrease in uterine weights ($P < 0.05$ on days 3, 7, and 14 *versus* control). In contrast, the uteri of the Tam-treated animals were hyperplasic and weighed significantly more than those of the control animals ($P < 0.001$ and $P < 0.05$ on day 3 and day 7, respectively, *versus* control). This is consistent with the fact that Tam has an agonistic effect on the endometrium in mice.

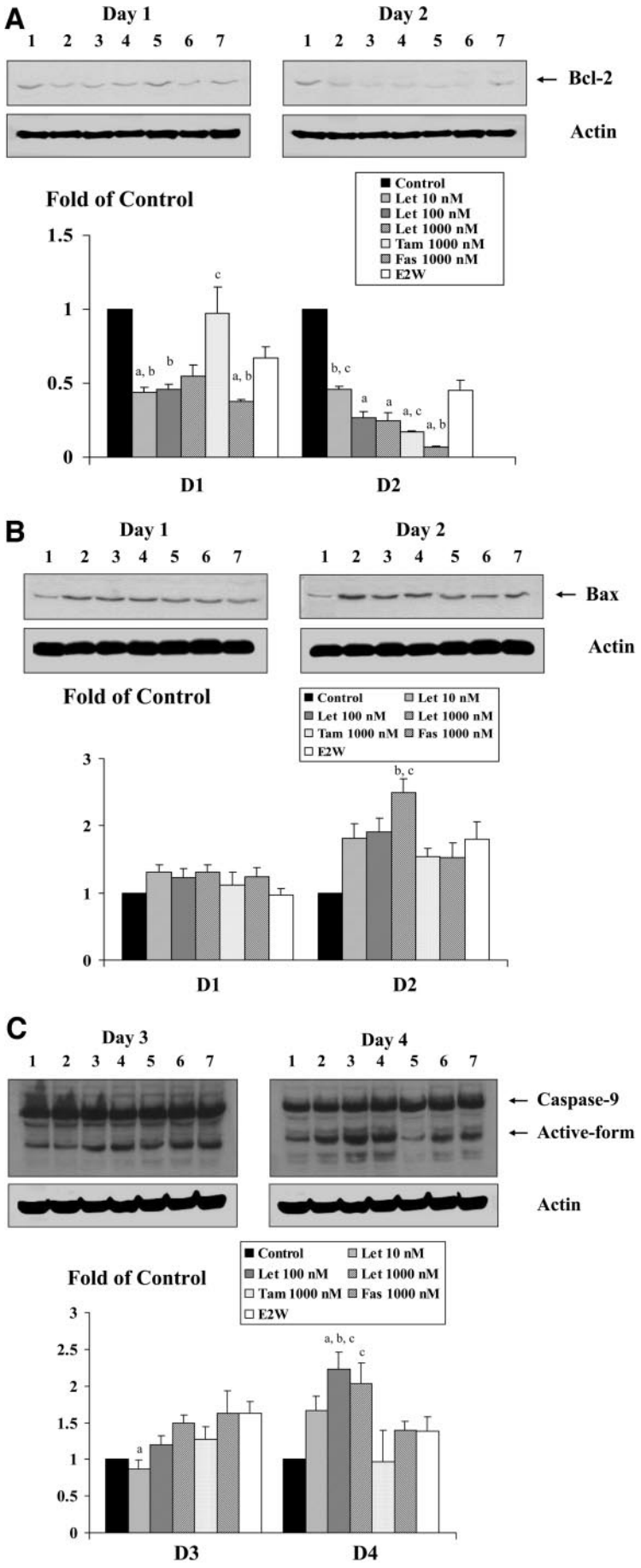

Fig. 3. Western immunoblotting analysis of whole cell lysates from MCF-7Ca cells cultured *in vitro* for *A*, Bcl-2 protein expression at M_r 26,000, *B*, Bax protein expression at M_r 26,000, and *C*, caspase-9 protein expression (proform at M_r 46,000 and active-form at M_r 35,000). Experimental protocol was as described in "Materials and Methods." *Lane 1*, control [AD (25 nM)]; *Lane 2*, Let (10 nM) +AD (25 nM); *Lane 3*, Let (100 nM) + AD (25 nM); *Lane 4*, Let (1000 nM) + AD (25 nM); *Lane 5*, 4-OHTam (1000 nM) + AD (25 nM); *Lane 6*, Fas (1000 nM) + AD (25 nM); *Lane 7*, E2W (vehicle, without AD). Blots were stripped and probed for β-actin (*bottom panel*) to verify equal amount of protein loaded in each lane. *a*, statistically different *versus* E2W; *b*, statistically different *versus* Tam; *c*, statistically different *versus* Fas ($P < 0.05$).

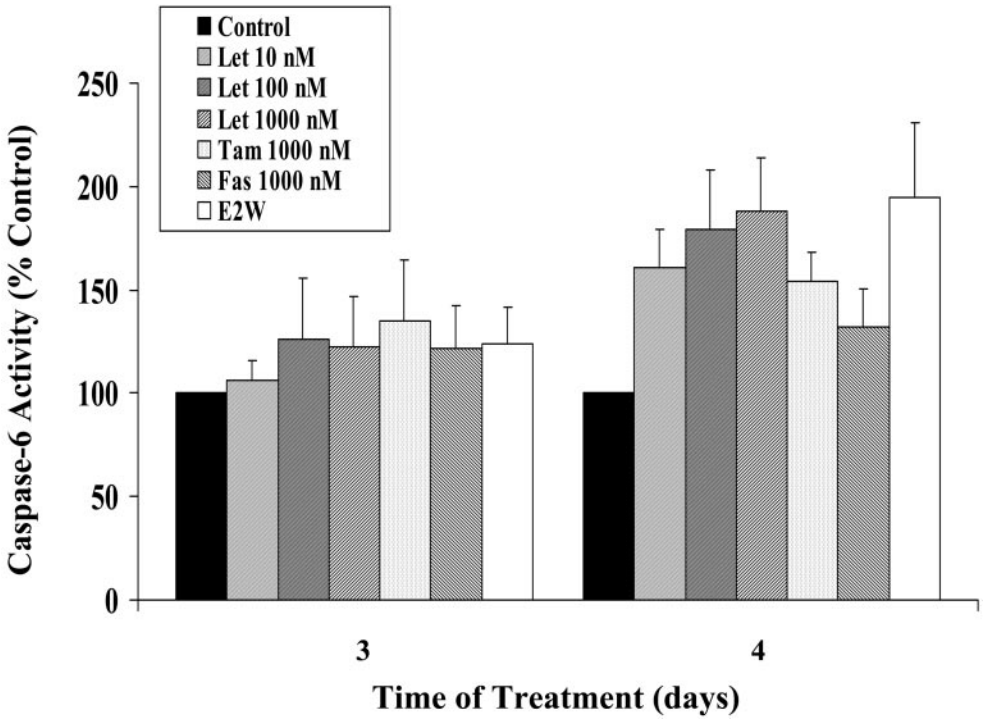

Fig. 4. Caspase-6 activity assay. MCF-7 Ca cells were cultured in steroid-free medium with the indicated treatments. The cell lysates were prepared as described in "Materials and Methods." One hundred μg of cell lysates were used for assay. After adding the reaction buffer and VEID-*p*NA (caspase-6 substrate), the samples were incubated at 37°C for 1 h. The absorbance of the samples was then read at 405 nm. Increases in caspase-6 activity were calculated as percentage of $A_{405\ nm}$ *versus* controls. Results are shown as the mean value from five independent experiments ± SE.

Detection of Apoptosis in MCF-7Ca Tumors Grown in Female Ovariectomized Nude Mice. To determine whether the apoptosis induced by aromatase inhibitors and antiestrogens in MCF-7Ca cells *in vitro* also occurred in MCF-7Ca tumors grown *in vivo*, we used two approaches to examine their effects. The first approach used *in situ* TUNEL staining to detect fragmented DNA indicative of cells undergoing apoptosis. TUNEL staining of control tumors revealed a low incidence of apoptosis with the apoptotic index range from 0.4 to 2.1% apoptotic cells (Fig. 6, *A* and *B*). The induction of apoptosis detected in the Let-treated tumors was dose- and time-dependent manner, which peaks at 14.5% ($P = 0.023$ *versus* control) and 15.8% ($P = 0.039$ *versus* control) on day 3 of treatment for Let 10 and 100 μg/day, respectively. Although the induction of apoptosis by Let was sustained for the duration of the experiment, the percentage of apoptotic cells declined with the longer treatment (5.5 and 9.9% apoptotic cells on day 14 for Let 10 and 100, respectively). E2W tumors showed a similar pattern as Let-treated tumors but with lower percentage of apoptosis. Although we did not observed significant reduction in tumor volumes, Tam and Fas also induced apoptosis of 5.0% ($P = 0.03$ *versus* control) and 5.5% ($P = 0.024$ *versus* control) on day 3 of treatment but decreased to 2.1 and 4.9% on day 14 of treatment.

The second approach to detect the early events of apoptosis was by observing the proteolysis of PARP, the DNA repair enzyme that can be cleaved by effector caspases. Western immunoblotting for the PARP protein revealed a reduction in the levels of the intact form (M_r 116,000) along with an elevation in the levels of the proteolytic form (M_r 85,000) in tumors treated with Let, Tam, Fas, and E2W (Fig. 7*A*). On Day 3, levels of the proteolytic form of PARP in tumors treated with Let (10 and 100 μg/day) and E2W were slightly increased to 1.25-, 1.29-, and 1.12-fold of control, respectively. The maximum level of proteolysis was achieved on day 7 of treatment when compared with control tumors, the proteolytic form of PARP was increased significantly ($P < 0.05$) by 4.82- and 29.25-fold in the Let 10 and Let 100, respectively. Levels were also significantly higher than in E2W tumors. On day 14, the levels of cleaved PARP were 4.11-, 9.54-, and 1.59-fold higher compared with control. In the Tam and Fas-treated tumors, levels of the proteolytic form of PARP were increased 2.68- and 4.49-fold on day 7 and 1.59- and 2.01-fold but not significantly compared with control on day 14 of treatment, respectively. This result was in agreement with the apoptotic index data obtained from the TUNEL assays *in vitro* and *in vivo*.

Activation of Caspase-9 and Caspase-7 in MCF-7Ca Tumors Grown in Nude Mice. Tumors were analyzed for expression of the active forms of caspase-9 and caspase-7. In agreement with the *in vitro* study, caspase-9 was also activated in MCF-7Ca tumors treated with Let, Tam, Fas, and E2W but not in control tumors (Fig. 7*B*). Maximal activation of caspase-9 occurred at day 3 of treatment. Proteolysis of PARP in MCF-7Ca tumors treated with Let, Tam, Fas, and E2W indicated the involvement of another effector caspase than caspase-6, which does not cleave PARP. Nuclear lamins has been reported to be the major substrate of caspase-6 (23). Caspase-3 is believed to be the major protease that functions in cleavage of PARP. Having found that caspase-3 is not activated in MCF-7Ca cells treated with aromatase inhibitors and antiestrogens, we assayed for expression of caspase-7, which has also been reported to cleave PARP (23, 24). Fig. 7*C* shows a marked significant activation of caspase-7 in Let-treated MCF-7Ca tumors. The protein expression of the cleaved active-form (M_r 20,000) of caspase-7 was increased in the Let-treated tumors in a dose- and time-dependent manner. The protein level of the proenzyme form (M_r 35,000) was gradually decreased in correlation with an increase in the cleaved form of caspase-7. Tumors from animals treated by estrogen withdrawal also showed activation of caspase-7. The protein level of the active-form in the E2W tumors was also increased in a time-dependent manner but to a significantly lesser extent than in the Let-treated tumors. The active form of caspase-7 was also increased in the Tam-treated tumors to about the same extent as E2W tumors, although we did not detect a significant number of apoptotic cells in this group. Interestingly, no active form of caspase-7 was detected in the Fas-treated tumors, although we did find PARP proteolysis and apoptotic cells in this group.

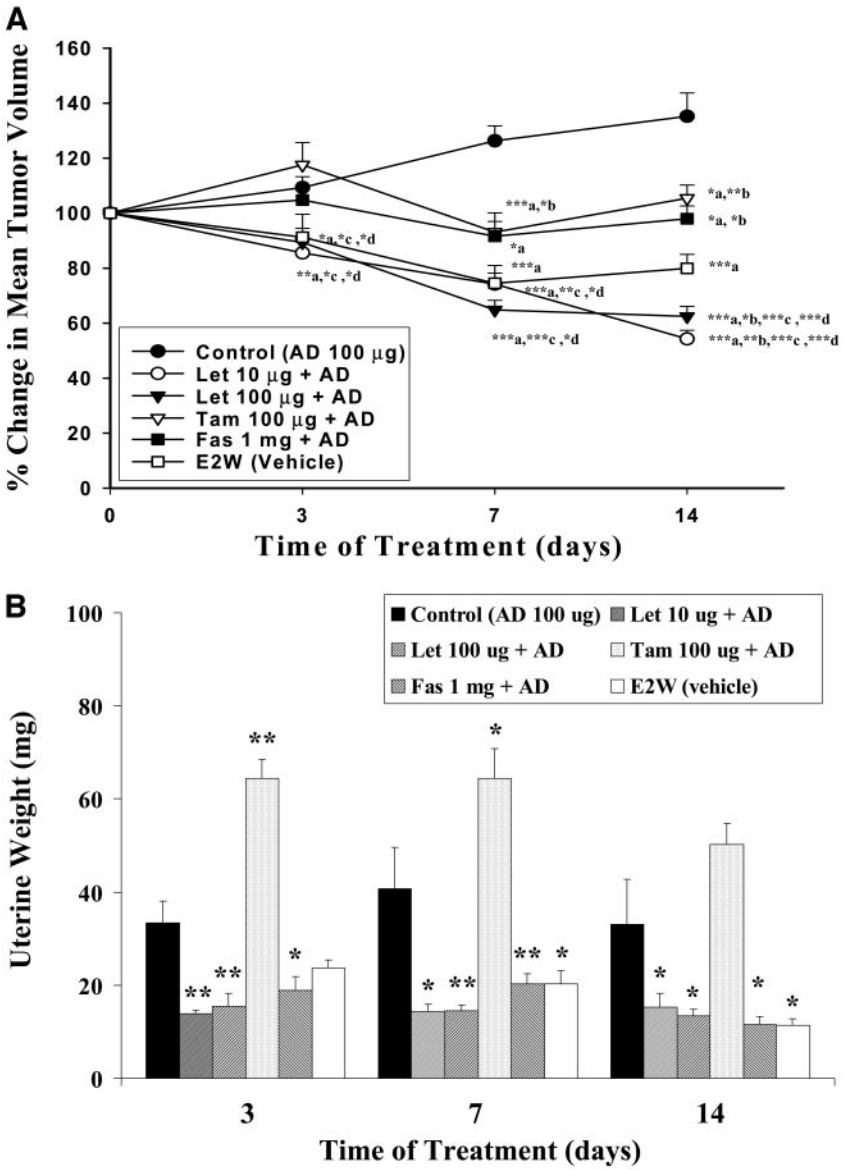

Fig. 5. The *in vivo* effects of Let, Tam, Fas, and E2W compared with control on MCF-7Ca tumors grown in female ovariectomized nude mice. Mice received two MCF-7Ca cells inoculations on each flank (2.5×10^6 cells/inoculation). Animals were injected s.c. daily with AD (100 μg/day) for the duration of treatment. When tumor volume was ~300 mm^3, animals were grouped ($n = 6$ for each group in each treatment time) for treatment with Let, Tam, and Fas. Control animals received only AD and E2W animals had AD withdrawn and were injected with vehicle. *A*, tumor volumes were measured on day 3, day 7, and day 14 of treatment. The values are expressed as a percentage of change in mean tumor volume/animal ($n = 6$) compared with day 0 of treatment ± SE. *, $P < 0.05$; **, $P < 0.005$, ***, $P < 0.0005$ (*a*, *versus* control; *b*, *versus* E2W; *c*, *versus* Tam; *d*, *versus* Fas). *B*, mean uterine weight. At the end of the experiment, the animals were sacrificed, and the tumors and uteri were removed, cleaned, and weighed. The values are expressed as mean uterine weight ($n = 6$) ± SE. *, $P < 0.05$; **, $P < 0.001$ *versus* control at each time point.

Up-Regulation of p53 and p21 Protein Levels in MCF-7Ca Cells and Tumors. After seeing that aromatase inhibitors and antiestrogens induced cell cycle arrest at G_0-G_1 phase, we additionally investigated the molecular mechanisms involved by focusing on the molecules that regulate at the G_1-S-phase transition. One critical regulator of both apoptosis and cell cycle is p53. The tumor suppressor protein p53 blocks cell cycle progression at the G_1-S transition (25). Levels of p53 protein expression in MCF-7Ca cells were not altered after treatments *in vitro* (Fig. 8*A*). However, we did observe significant up-regulation in expression of p53 protein in MCF-7Ca tumor xenografts (Fig. 8*C*). Compared with control tumors, the high dose of Let (100 μg/day) induced a 3.25-fold increase in p53 protein levels on day 3 of treatment. On day 7 and day 14 of treatment, the induction declined to 1.56- and 1.23-fold of control, respectively. Up-regulation of p53 protein expression by the low dose of Let (10 μg/day) occurred at a later time than was observed with Let (100 μg/day). Significantly increased p53 protein levels were detected on day 7 (2.56-fold) and remain high on day 14 of treatment (2.06-fold). Significant up-regulation of p53 by Tam peaked on day 3 (2.91-fold), whereas Fas induced p53 expression by 2.45-fold of control on day 7 of treatment. In the E2W tumors, we observed a slight and transient increase in p53 levels (1.69-fold of control) on day 3 of treatment.

In addition, we also examined the effects of aromatase inhibitors and antiestrogens on expression of the p21 protein both *in vitro* and *in vivo*. Levels of p21 protein of MCF-7Ca cells were increased in all treatments compared with control. Let induced up-regulation in expression of p21 protein in a dose- and time-dependent manner (Fig. 8*B*). Although higher levels of p21 protein expression were induced by Let (10 μM), at equivalent concentrations of 1 μM, there was no significant difference between p21 protein expression in Let-, 4-OH-Tam-, and Fas-treated cells. In agreement with *in vitro* results, expression of p21 protein is also significantly up-regulate in MCF-7Ca tumors after treatment of Let compared with control, E2W, and antiestrogens (Fig. 8*D*). On day 7 of treatment, Let (10 and 100 μg/day) increased p21 protein expression by 9.36- and 3.48-fold of control, respectively. This effect was maintained through day 14 of treatments with increases of 3.73- and 3.34-fold of control. Up-regulation of p21 protein expression was also observed on day 7 in Fas-treated tumors when increase in p21 protein levels were 4.07-fold of control but returned to the control level on day 14 of treatments.

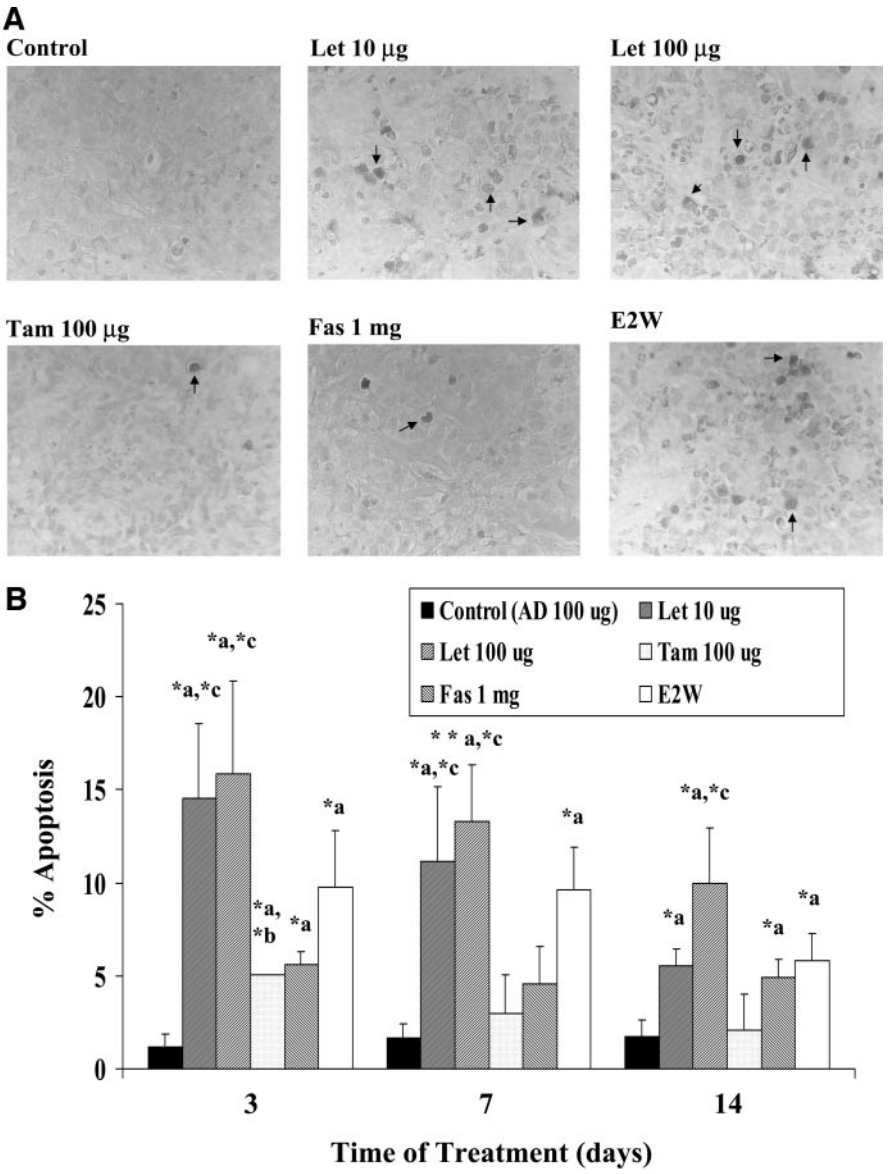

Fig. 6. Induction of apoptosis in MCF-7Ca tumors grown in female ovariectomized nude mice. *A, in situ* detection of cells undergoing apoptosis by TUNEL staining; *arrowheads* point to apoptotic cells (black-stained cells), counterstaining was with methyl green. Sections were representative of tumors from day 7 of treatment. *B*, percentage of apoptotic cells in MCF-7Ca tumors treated with Let (10 μg/day), Let (100 μg/day), Tam (100 μg/day), or Fas (1 mg/day) for 3, 7, and 14 days compared with control and E2W tumors. Graph shows mean values in each group, $n = 4$ (*bars*, $\pm$SE). *a*, statistically different *versus* control; *b*, statistically different *versus* E2W; *c*, statistically different *versus* Tam; Fas was not significantly different from other treated groups in correlated time of treatment (*, $P < 0.05$; **, $P < 0.01$).

Only a slight increase of p21 protein expression was evident in E2W and Tam-treated tumors (1.31- and 1.35-fold of control, respectively, on day 7 of treatments).

Modulation in the Expression of Genes Involved in Apoptosis and Cell Cycle Regulation. To further characterize the molecular mechanisms associated with the antiproliferative effects and induction of apoptosis induced by aromatase inhibitors and antiestrogens, we examined changes in the expression of genes involved in these processes. We used the RPA method using the RiboQuant Multiprobe protection assay system to simultaneously detect and quantify levels of expression of multiple mRNA species. On the basis of our preliminary *in vitro* results, we selected to examine expression of *bcl-2*, *bax*, *PARP*, *caspase-3*, *caspase-6*, *caspase-7*, *caspase-8*, *caspase-9*, *p53*, *p21*, *cyclin D1*, *PCNA*, and *c-myc* genes in MCF-7Ca breast tumor xenografts. In MCF-7Ca tumors treated with Let 10, Let 100, Tam, Fas, and E2W for 3 days, *bax* mRNA levels were increased by 1.13-, 1.23-, 1.34-, 1.36-, and 1.56-fold of the control, respectively. The increase in the levels of *bax* mRNA was transient because levels similar to those in the control tumors had returned on day 7 and day 14 of treatment. For *bcl-2*, a significant decrease in mRNA levels was found in Let 10 and Let 100 tumors with the peak of reduction on day 7 of treatment. On day 7, the levels of *bcl-2* mRNA in Let 10 and 100 were 0.73- and 0.65-fold of control and were at the same level on day 14 of treatment. No alteration of *bcl-2* mRNA level was detected on day 3 and day 7 for E2W-, Tam-, or Fas-treated tumors. However, on day 14, the level of *bcl-2* mRNA in E2W tumors had dropped to 0.64-fold of control. On day 14, a slight decrease in expression of *bcl-2* mRNA to 0.9-fold of control was detected in Tam- and Fas-treated tumors (data not shown).

Quantitative analysis of *caspase-6*, *caspase-7*, *caspase-8*, and *caspase-9* mRNA expression showed no significant change in the levels of these genes in the MCF-7Ca-treated tumors. There was also no significant increase in the expression of *PARP* mRNA after treatment with Let, Tam, Fas, or E2W. In contrast, there was a significant reduction in the level of *c-myc* mRNA. Let treatment of MCF-7Ca tumors resulted in a dramatic decrease in levels of *c-myc* mRNA. The reduction in *c-myc* mRNA expression started on day 3 and was prolonged through day 7 and day 14 of treatment (Fig. 9). Expression of *c-myc* mRNA also gradually decreased in the Tam-, Fas-, and E2W-treated tumors, but the time course was later than in the Let-treated tumors. On day 14 of treatment, the levels of c-myc mRNA in all treatment groups were almost undetectable.

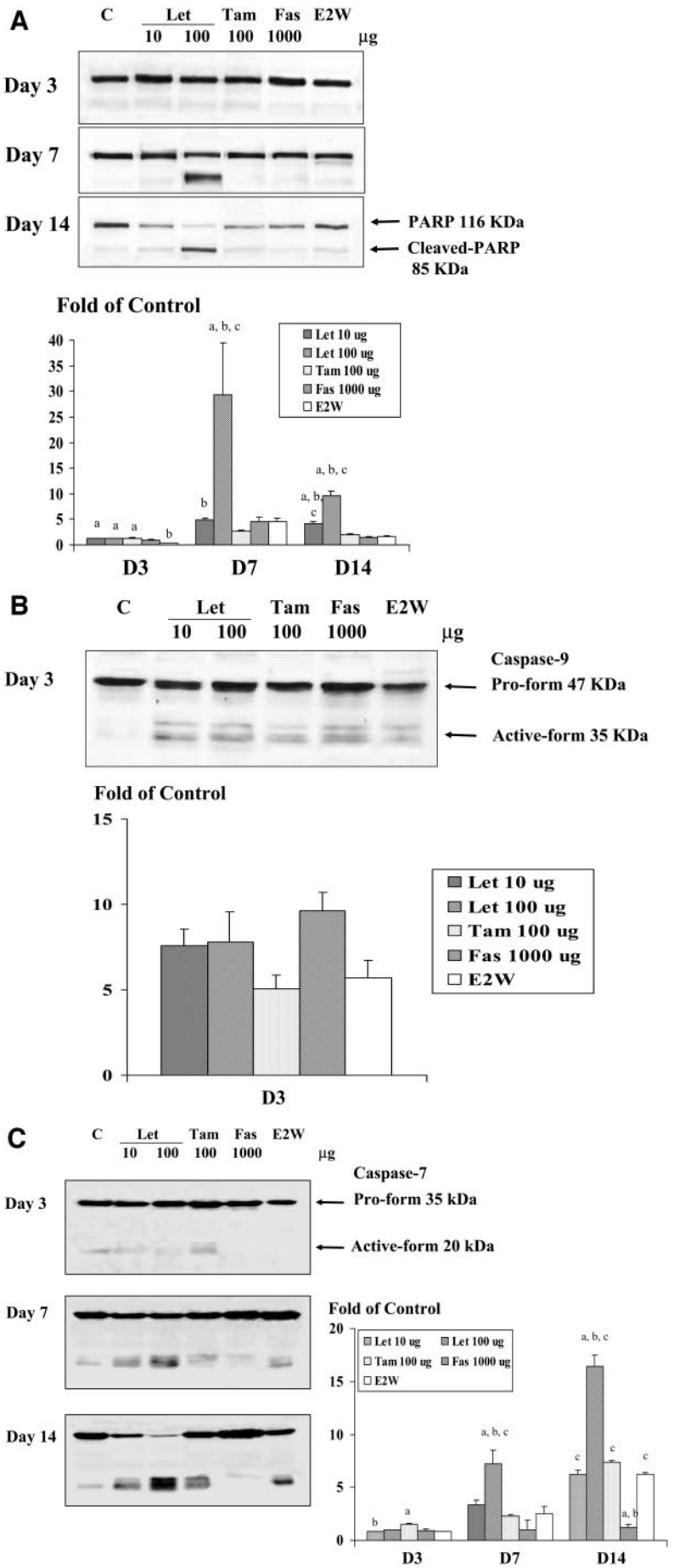

Fig. 7. *A*, Proteolysis of PARP in MCF-7Ca tumors grown in female ovariectomized nude mice. Western immunoblotting analysis of PARP protein expression in MCF-7Ca tumors treated with Let (10 μg), Let (100 μg), Tam (100 μg), Fas (1 mg), and E2W (vehicle) compared with control for 3, 7, and 14 days. At the indicated time points, the animals were sacrificed, and tumors were excised, cleaned, and weighed before storage at −80°C. Tumors were homogenized in lysis buffer. Fifty μg of total protein were subjected to SDS-PAGE, transferred to a nitrocellulose membrane before immunoblotting with anti-PARP antibodies that recognized both intact PARP at M_r 116,000 and proteolytic PARP at M_r 85,000. *B*, activation of caspase-9 in MCF-7Ca tumors. Western immunoblotting analysis of caspase-9 protein expression in MCF-7Ca tumors treated with Let (10 μg), Let (100 μg), Tam (100 μg), Fas (1 mg), and E2W (vehicle) compared with control for 3 days. Results of immunoblotting with anti-caspase-9 antibodies that recognized proform at M_r 35,000 and cleaved active form at M_r 20,000 are shown. *C*, activation of caspase-7 in MCF-7Ca tumors. Western immunoblotting analysis of caspase-7 protein expression in MCF-7Ca tumors treated with Let (10 μg), Let (100 μg), Tam (100 μg), Fas (1 mg), and E2W (vehicle) compared with control for 3, 7, and 14 days. Results of immunoblotting with anticaspase-7 antibodies that recognized proform at M_r 35,000 and cleaved active form at M_r 20,000 are shown. Results are shown from a single representative of three independent experiments. *a*, statistically different *versus* E2W; *b*, statistically different *versus* Tam; *c*, statistically different *versus* Fas ($P < 0.05$).

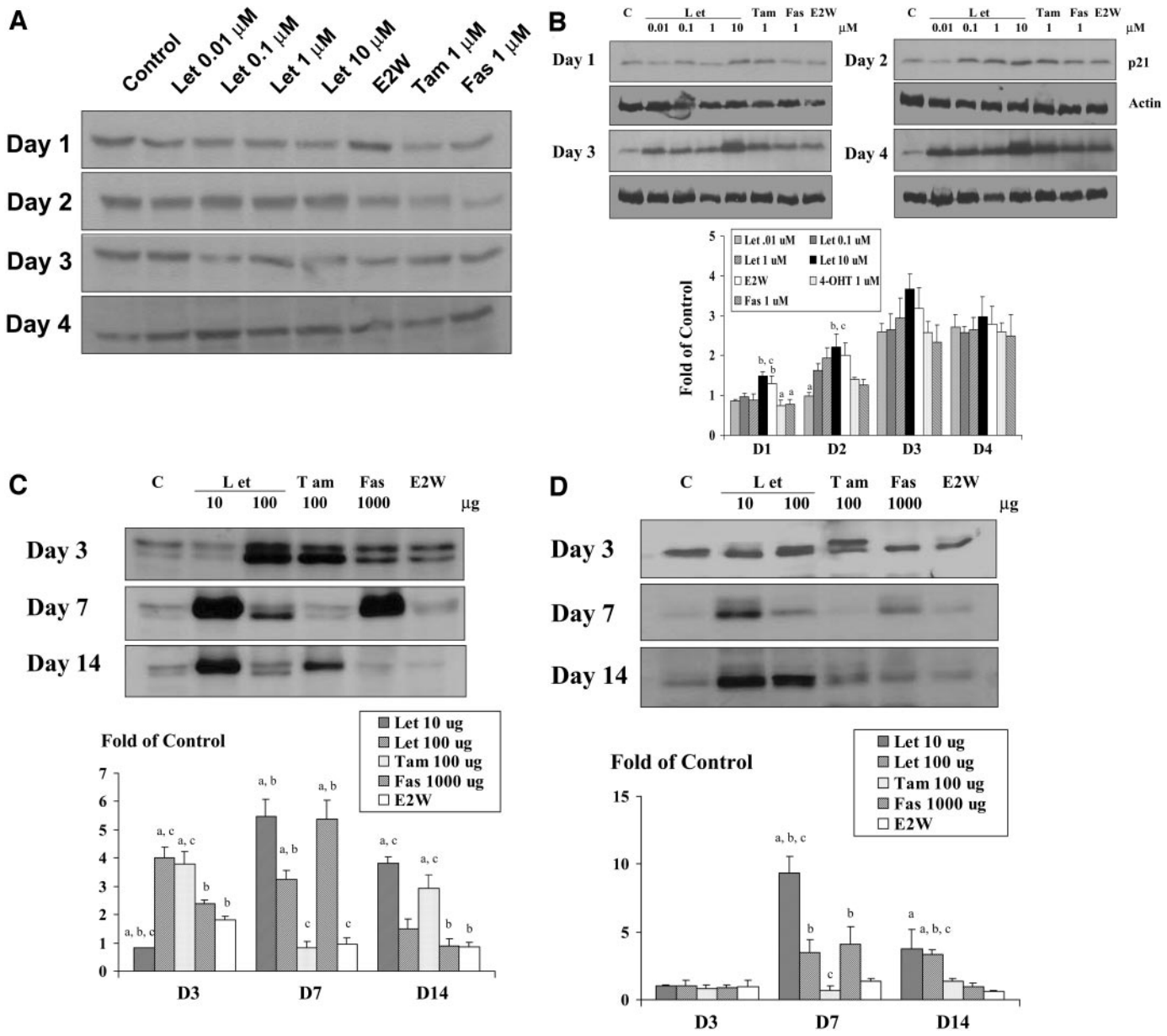

Fig. 8. Western immunoblotting analysis of whole cell lysates for *A*, p53 protein expression from MCF-7Ca cells cultured *in vitro*, *B*, p21 protein expression from MCF-7Ca cells cultured *in vitro*, *C*, p53 protein expression from MCF-7Ca tumors, and *D*, p21 protein expression from MCF-7Ca tumors. Experimental protocol was as described in "Materials and Methods." *a*, statistically different *versus* E2W; *b*, statistically different *versus* Tam; *c*, statistically different *versus* Fas ($P < 0.05$).

Reduction in *cyclin D1* and *PCNA* mRNA levels were also observed in MCF-7Ca tumors treated with Let, Tam, Fas, and E2W, and these reductions occurred in a time-dependent manner. Compared with the control, levels of *cyclin D1* mRNA were reduced by 0.73-, 0.66-, 0.57-, 0.72-, and 0.86-fold, and PCNA mRNA levels were reduced by 0.61, 0.48, 0.46, 0.60, and 0.75-fold on day 14 of treatment with Let 10, Let 100, Tam, Fas, and E2W, respectively (Fig. 9). The levels of *p53* mRNA were increased in MCF-7Ca tumors treated with Let, Tam, Fas, and E2W for 3 days before gradually returning to the basal level on day 14 of treatment. A similar profile was also seen for *p21* mRNA (Fig. 9).

DISCUSSION

The aim of this study was to explore the molecular mechanisms associated with the antiproliferative effect of aromatase inhibitors in comparison with antiestrogens for the treatment of breast cancer. By culturing aromatase-transfected MCF-7Ca cells in steroid-free medium supplemented with AD, we were able to test the *in vitro* effects of both the aromatase inhibitors and antiestrogens on cell growth, cell cycle progression, and induction of apoptosis. Our results indicated that aromatase inhibitors, antiestrogens, and E2W treatment induced inhibition of MCF-7Ca cell proliferation. However, the growth inhibitory effect of aromatase inhibitors was superior compared with antiestrogens (Tam and Fas) or E2W. This has also been demonstrated in recent clinical trials where Let and Anas were more effective in comparison with Tam (17, 26). In addition, using our *in vivo* intratumoral aromatase nude mouse model, we found that Let induced regression of MCF-7Ca tumors, whereas tumor growth arrest was observed in the Tam- and Fas-treated tumors. These results suggest that at least in our tested system, the inhibition of estrogen synthesis by an aromatase inhibitor is more effective than inhibiting the action of estrogen with an antiestrogen. These findings are consistent with

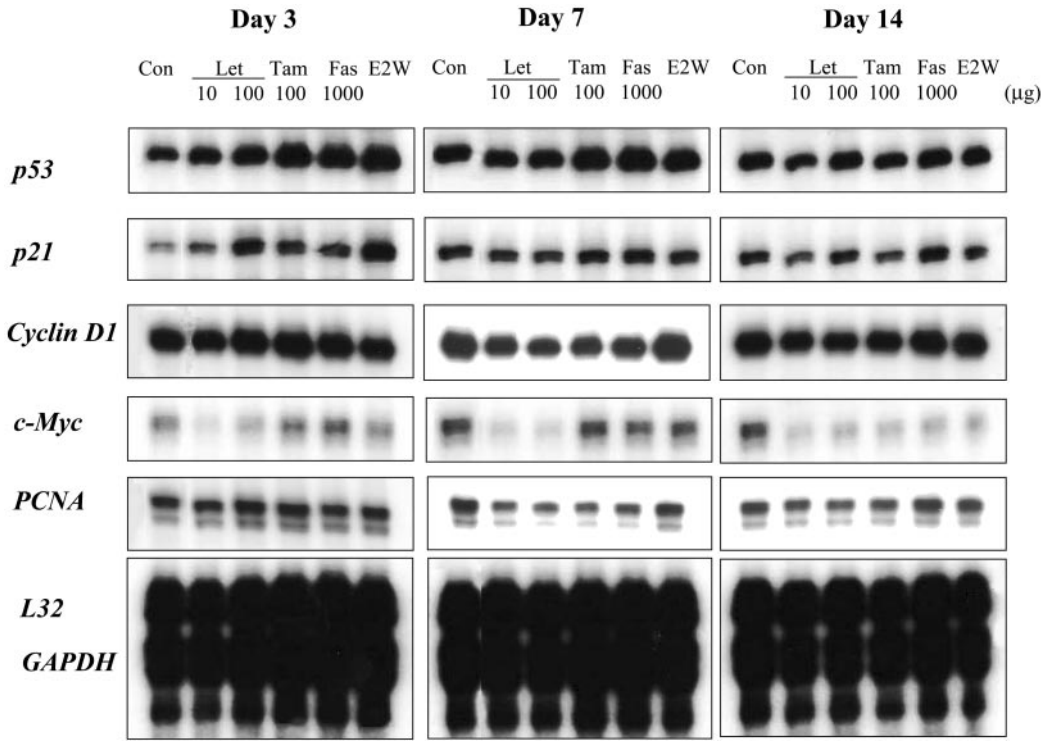

Fig. 9. Alteration in expression of apoptotic and cell cycle regulatory genes in MCF-7Ca tumors grown in female ovariectomized nude mice. MCF-7Ca tumors xenografts in nude mice were treated for 3, 7, and 14 days with Let (10 and 100 μg/day), Tam (100 μg/day), or Fas (1 mg/day) in addition to AD (100 μg/day) supplement. Control mice received s.c. injections of AD only. E2W mice were administrated with vehicle (0.3% hydroxyl propyl cellulose, 0.1 ml/day) without AD supplement. At the indicated time period, animals were sacrificed, and tumors were harvested, weighed, and stored in RNAlater solution at -80°C. Total RNA was isolated and 20 μg of RNA were subjected to RPA as described in "Materials and Methods." Autoradiographic of *p53*, *p21*, *cyclin D1*, *c-myc*, and *PCNA* mRNA. Levels of *L32* and *GAPDH* mRNA in corresponding lanes were served as an internal control for each assay. Results are shown from a single representative of three independent experiments.

our previous studies using this model (27, 28). The xenograft model is similar to the postmenopausal breast cancer patient in several respects. Aromatase is expressed in nonovarian tissue and is not regulated by gonadotropins. Although circulating levels of estrogen are low in postmenopausal women, the concentrations of estrogen in the breast are similar to premenopausal levels (29–31), in part, because of steroid uptake and, in part, because of local synthesis via aromatase expressed in stromal cells, tumor epithelial cells, and adipocytes (32, 33). Although expression of aromatase is limited to the tumor cells in the xenograft model and estrogen concentrations may be relatively high compared with patients, systemic aromatase inhibitor treatment will inhibit estrogen synthesis in all sites and reduce the amount taken up as well as that produced locally. It would seem logical that wherever estrogen is produced, the determining factor would be the amount of estrogen available to the tumor cell's ERs. An advantage of this xenograft model is that because tumor cells are ER positive and express aromatase, both antiestrogens and aromatase inhibitors can be studied. Although androstenedione is provided as a supplement because the adrenal hormones are deficient in the nude mice (34), there are no direct effects on tumor growth (16, 21).

Estrogens exert their proliferative effect on hormone-dependent breast cancer cells by stimulating cell cycle progression. Studies have been shown that antiestrogen treatment or estrogen deprivation prevents MCF-7 cells entering into S phase of the cell cycle (12, 35). We demonstrate here that both aromatase inhibitors and antiestrogens induce growth arrest of MCF-7Ca cells by blocking the G_1-S-phase transition of cell cycle. Preventing entry into S phase subsequently led to a decrease in the percentage of cells in S and M phase. Tumor growth rate is dependent on both proliferation rate and apoptotic rate. In addition to inducing cell cycle progression, estrogens are known to protect against cell death by apoptosis. Several studies both *in vitro* and *in vivo* have reported that Tam, Fas, and E2W induce apoptosis (10, 12, 36). Using MCF-7Ca cells culture *in vitro* and *in vivo* growth in nude mouse, this is the first study to compare the efficacy of aromatase inhibition by Let, Anas, and 4-OHA to 4-OHTam, Fas, and E2W to induce apoptosis. Our results indicate that aromatase inhibitors have higher efficiency in inducing apoptosis than antiestrogens and E2W. Among all of the treatments, Let was shown to be the most effective at inducing apoptosis. Moreover, the order of potency of the aromatase inhibitors at inhibiting cell proliferation, cell cycle arrest, and apoptotic induction was Let $>$ Anas $>$4-OHA. It is possible that the differences in efficacies of the three aromatase inhibitors resulted from differences in their abilities to inhibit aromatase activity. We have previously reported that in several aromatase-expressing cell lines, including MCF-7Ca, Let is more effective than Anas and 4-OHA at inhibiting aromatase activity (37). It should be noted that apoptosis observed in MCF-7Ca tumors treated with Let, Tam, Fas, and E2W was maintained through 14 days of treatment but the maximal induction was at day 3 of treatment. It was unexpected that Let was more effective than E2W. Whether it reflects other actions of the compound is unknown and will require additional investigation.

Previous studies have indicated that E_2 protects against breast cancer cell death by apoptosis is associated with increased levels of the antiapoptotic Bcl-2 protein. Our results here demonstrate that the induction of apoptosis in MCF-7Ca cells by Let, 4-OHT, Fas, and E2W is associated with a reduction in the levels of Bcl-2. The mechanisms responsible for up-regulation of Bcl-2 by E2 are not fully understood but likely involved the interaction of E_2 with ER (38). In breast carcinomas, Bcl-2 expression has been shown to correlate with ER status (39). It has been reported that E_2 up-regulates the *bcl-2* mRNA level in MCF-7 cells and that the mechanism is via ER binding

to two estrogen response elements located within the *bcl-2* coding region (40). It has also been shown that Tam-induced apoptosis in MCF-7 cells involves down-regulation of Bcl-2 but not Bax (41). In this study, we found up-regulation of proapoptotic protein Bax accompanied with down-regulation of antiapoptotic protein Bcl-2 after all treatments. The modulation in levels of Bcl-2 and Bax was concomitant and were observed as early as day 1 of treatments. Collectively, down-regulation of an antiapoptotic protein together with up-regulation of a proapoptotic protein would be expected to produce a more powerful response and a greater induction of apoptosis. It is well established that Bcl-2 and Bax acts upstream of apoptotic mitochondrial pathway (42). Decreasing of Bcl-2/Bax ratio leads to opening of mitochondrial permeability transition pores and the release of cytochrome *c* (43). Cytochrome *c* interacts with Apaf-1 and dATP (or ATP) and promotes the proteolytic activation of the caspase-9 zymogen (44). Activated caspase-9 then initiates a cascade activation of downstream caspases-3, -7, -2, -6, -8, and -10 (45). We detected the activation of caspase-9 on day 3 and day 4 of treatments with hormonal therapies, which is after the peak of modulation in Bcl-2 and Bax expression. Our results suggest that Bcl-2 and Bax are critical in the early events of apoptosis induced by Let, Tam, and Fas. MCF-7 cells, the parent cell line of MCF-7Ca cells, are known to have lost functional caspase-3 expression because of a 47-bp deletion within exon 3 of the *caspase-3* gene (19, 20). Caspase-3 is believed to be the major executioner caspase downstream of caspase-9. In agreement with the published data using MCF-7 cells, we did not see activation of caspase-3 in MCF-7Ca cells with any of the treatments. This is most likely because MCF-7Ca cells also lack functional caspase-3.

Initiator caspases such as caspase-9 or caspase-8 can activate the apoptotic pathway not only by activating caspase-3 but also through activation of caspase-7 (46–48). Moreover, *in vitro* studies have shown that caspase-3 and caspase-7 have very similar substrate specificity, one of which is PARP (24). Additional studies using a cell-free systems and caspase-3-deficient cells from *CASP-3*-knockout animals have reported that in absence of caspase-3, PARP is cleaved by caspase-7 (49, 50). In the present study, we observed the activation of caspase-7 in MCF-7Ca tumors treated with Let, Tam, and E2W but not in tumors treated with Fas. Additionally, levels of the active-cleaved form of caspase-7 were correlated with levels of PARP cleavage and an increased in apoptotic index. We also demonstrated that caspase-6 is activated after treatment with Let and E2W and to a lesser extent by Tam and Fas. Activation of caspase-9 and caspase-7 and the inactivation of PARP correlated with a reduction in expression of the proforms of these enzymes. Analysis of the RPAs indicated that there was no induction in the mRNA levels of *caspase-8*, *caspase-9*, *caspase-6*, *caspase-7*, and *PARP*. These results suggested that the activation of caspases observed in our studies is likely to be regulated at the protein level rather than at the transcription level.

E_2-induced cell cycle G_1-phase progression is mediated by activation of Cdk4 and Cdk2 via increased expression of its regulatory subunit, cyclin D1, and decreased association to Cdk inhibitor p21 (7). It has been reported that Fas induces expression of p21 protein and mRNA (51) and that E_2 deprivation up-regulates expression of p21 but not cyclin D1 (12). The tumor suppressor protein p53 is a key regulator of cell cycle progression and apoptosis (52). As a transcription factor, p53 increases transcription expression of several genes, including *p21* and *bax* (53), and inhibits the expression of *bcl-2* by binding to the silencer element in the *bcl-2* gene (54). Here, we demonstrated that the inhibition of cell cycle progression in associated with the hormonal treatment of MCF-7Ca cells correlates with a decrease in *cyclin D1* mRNA levels and an increase in the expression of p53 and p21 protein and mRNA levels. We also observed a reduction in *c-myc* mRNA levels in the tumors treated with Let, antiestrogens, or E2W. Increased *c-myc* transcription and protein levels are an early response to treatment with E_2. E_2 activates *c-myc* expression via the interaction of the E_2-ER complex with a 116-bp estrogen response element in the *c-myc* promoter (55). The oncoprotein *c-myc* induces cell proliferation by promoting a G_1-S-phase transition. One mechanism of which is by increasing the transcription of the phosphatase Cdc25A, which is required for activation of cyclin-Cdk complexes in the cell cycle machinery (56). Studies by others showed that reduction of c-myc expression is followed by activation of cyclin-dependent kinase inhibitor p27, which induces growth arrest and apoptosis (57). Interestingly, it has been reported that cyclin D1-deficient mice remain fully sensitive to the oncogenic pathway driven by *c-myc* (58). This implied different mechanisms of *cyclin D1* and *c-myc* in regulation of cell growth. Therefore, the marked and rapid decrease in expression of both *cyclin D1* and *c-myc* induced by Let should give some advantage for breast cancer treatment.

To the best of our knowledge, this is the first study documenting the mechanisms and signaling pathways regulating cell cycle and induction of apoptosis upon treating breast cancer cells with aromatase inhibitors in comparison with antiestrogens. Our results indicate that aromatase inhibitors and antiestrogens inhibit the proliferation of MCF-7Ca breast cancer cells by inducing cell cycle arrest in the G_0-G_1 phase, and this is coupled with increased apoptosis. The apoptotic signaling pathways induced involves down-regulation of Bcl-2, up-regulation of Bax, and the activation of caspase-9, caspase-6, and caspase-7. The mechanisms responsible for cell cycle arrest are associated with up-regulation of p53 and p21 protein and mRNA levels concomitant with down-regulation of *cyclin D1* and *c-myc* mRNA expression. Although the mechanisms involved appeared to be similar for antiestrogens and aromatase inhibitors, the most significant effects occurred with Let, which were greater than with E2W and consistent with marked effects of Let on tumor and cell growth.

ACKNOWLEDGMENTS

We thank Dr. Shiuan Chen for kindly providing MCF-7Ca cells, Dr. Dean Evans for Let, and Dr. Alan Wakeling for Anas and Fas. We also thank Danijela Jelovac, Venkatesh Handratta, and Ritesh Kataria for their expert assistance in tumor measurement and isolation. We thank Jane Michalski for technique advice in sequencing gel and Natalie Wehman for assistance with fluorescence-activated cell sorting and cell cycle analysis.

REFERENCES

1. Wang, T. T. Y., and Phang, J. M. Effect of estrogen and apoptosis pathways in human breast cancer cell line MCF-7. Cancer Res., *55:* 2487–2489, 1995.
2. Leung, L. K., Do, L., and Wang, T. T. Regulation of death promoter *bax* expression by cell density and 17β-estradiol in MCF-7 cells. Cancer Lett., *124:* 47–52, 1998.
3. Evan, G., and Littlewood, T. D. A matter of life and cell death. Science (Wash. DC), *281:* 1317–1322, 1998.
4. Kerr, J. F., Wyllie, A. H., and Currie, A. R. Apoptosis: a basic biological phenomenon with wide-ranging implications in tissue kinetics. Br. J. Cancer, *26:* 239–257, 1972.
5. Alnemri, E. S., Livingston, D. J., Nicholson, D. W., Salvesen, G., Thornberry, N. A., Wong, W. W., and Yuan, J. Human ICE/CED-3 protease nomenclature. Cell, *87:* 171, 1996.
6. Dragovich, T., Rudin, C. M., and Thompson, C. B. Signal transduction pathways that regulate cell survival and cell death. Oncogene, *17:* 3207–3213, 1998.
7. Prall, O. W. J., Sarcevic, B., Musgrove, E. A., Watts, C. K. W., and Sutherland, R. L. Estrogen-induced activation of Cdk4 and Cdk2 during G_1-S phase progression is accompanied by increased cyclin D1 expression and decreased cyclin-dependent kinase inhibitor association with cyclin E-Cdk2. J. Biol. Chem., *272:* 10882–10894, 1997.
8. Planas-Silva, M. D., and Weinberg, R. A. Estrogen dependent cyclin E-cdk2 activation through p21 redistribution. Mol. Cell. Biol., *17:* 4059–4069, 1997.
9. Lippman, M. E., and Dickson, R. B. Mechanisms of normal and malignant breast epithelial growth regulation. J. Steroid Biochem., *34:* 107–121, 1989.
10. Kyprianou, N., English, H. F., Davidson, N. E., and Isaacs, J. T. Programmed cell death during regression of the MCF-7 human breast cancer following estrogen ablation. Cancer Res., *51:* 162–166, 1991.

11. Wilson, J. W., Wakeling, A. E., Morris, I. D., Hickman, J. A., and Dive, C. MCF-7 human mammary adenocarcinoma cell death *in vitro* in response to hormone-withdrawal and DNA damage. Int. J. Cancer, *61:* 502–508, 1995.
12. Truchet, I., Jozan, S., Guerrin, M., Mazzolini, L., Vidal, S., and Valette, A. Interconnections between E2-dependent regulation of cell cycle progression and apoptosis in MCF-7 tumors growing on nude mice. Exp. Cell Res., *254:* 241–248, 2000.
13. Detre, S., Salter, J., Barnes, D. M., Riddler, S., Hills, M., Johnston, S. R., Gillett, C., A'Hern, R., and Dowsett, M. Time-related effects of estrogen withdrawal on proliferation and cell death-related events in MCF-7 xenografts. Int. J. Cancer, *81:* 309–313, 1999.
14. Brodie, A. M. H., and Njar, V. C. O. Aromatase inhibitors and their application in breast cancer treatment. Steroids, *65:* 171–179, 2000.
15. Brodie, A. M. H., Schwarsel, J. R., Shaikh, A. A., and Brodie, H. J. The effect of an aromatase inhibitor, 4-hydroxy-4-androstene-3,17-dione, on estrogen dependent processes in reproduction and breast cancer. Endocrinology, *100:* 1684–1694, 1977.
16. Yue, W., Wang, J., Savinov, A., and Brodie, A. Effect of aromatase inhibitors on growth of mammary tumors in a nude mouse model. Cancer Res., *55:* 3073–3077, 1995.
17. Mourindsen, H., Gershanovich, M., Sun, Y., Pérez-Carrión, R., Boni, C., Monnier, A., Apffelstaedt, J., Smith, R., Sleeboom, H. P., Jänicke, F., Pluzanska, A., Dank, M., Becquart, D., Bapsy, P. P., Salminen, E., Snyder, R., Lassus, M., Verbeek, J. A., Staffler, B., Chaudri-Ross, H. A., and Dugan, M. Superior efficacy of letrozole (Femara) *versus* tamoxifen as first-line therapy for postmenopausal women with advanced breast cancer: results of a Phase III study of the International Letrozole Breast Cancer Group. J. Clin. Oncol., *19:* 2596–2606, 2001.
18. Zhou, D., Pompon, D., and Chen, S. Stable expression of human aromatase complementary DNA in mammalian cells: a useful system for aromatase inhibitor screening. Cancer Res., *50:* 6949–6954, 1990.
19. Janicke, R. U., Sprengart, M. L., Wati, M. R., and Porter, A. G. Caspase-3 is required for DNA fragmentation and morphological associated with apoptosis. J. Biol. Chem., *273:* 9357–9360, 1998.
20. Kurakawa, H., Nishio, J. K., Fukumoto, H., Tomonari, A., Suzuki, T., and Saijo, N. Alteration of caspase-3 (CPP/Yama/Apopain) in wild type MCF-7 breast cancer cell. Oncol. Rep., *6:* 33–37, 1999.
21. Yue, W., and Brodie, A. M. H. A nude mouse model for postmenopausal breast cancer using MCF-7 cells transfected with the human aromatase gene. Cancer Res., *54:* 5092–5095, 1994.
22. Long, B. J., Jelovac, D., Thiantanawat, A., and Brodie, A. M. The effect of second-line antiestrogen therapy on breast tumor growth after first-line treatment with aromatase inhibitor letrozole: long-term studies using the intratumoral aromatase postmenopausal breast cancer model. Clin. Cancer Res., *8:* 2378–2388, 2002.
23. Nuñez, G., Benedict, M. A., Hu, Y., and Inohara, N. Caspases: the proteases of apoptotic pathway. Oncogene, *17:* 3237–3245, 1998.
24. Thornberry, N. A., Rano, T. A., Peterson, E. P., Rasper, D. M., Timkey, T., Garcia-Calvo, M., Houtzager, V. M., Nordstrom, P. A., Roy, S., Vaillancourt, J. P., Chapman, K. T., and Nicholson, D. W. A combinatorial approach defines specificities of members of the caspase family and granzyme B. Functional relationships established for key mediators of apoptosis. J. Biol. Chem., *272:* 17907–17911, 1997.
25. White, E. Life, death, and the pursuit of apoptosis. Genes Dev., *10:* 1–15, 1996.
26. Nabholtz, J. M., Buzdar, A., Pollak, M., Harwin, W., Burton, G., Mangalik, A., Steinberg, M., Webster, A., and von Euler, M. Anastrozole is superior to tamoxifen as first-line therapy for advanced breast cancer in postmenopausal women: results of a North American multicenter randomized trial. Arimidex Study Group. J. Clin. Oncol., *18:* 3758–3767, 2000.
27. Lu, Q., Liu, Y., Long, B. J., Grigoryev, D., Gimbel, M., and Brodie, A. The effect of combining aromatase inhibitors with antiestrogens on tumor growth in a nude mouse model for breast cancer. Breast Cancer Res. Treat., *57:* 183–192, 1999.
28. Long, B. J., Jelovac, D., Handratta, V., Thiantanawat, A., MacPherson, N., Ragaz, J., and Brodie, A. M. Therapeutic strategies using the aromatase inhibitor letrozole and tamoxifen in a breast cancer model. JNCI, in press, 2003.
29. Thorsen, T., Tangen, M., Stoa, K. F. Concentrations of endogeneous estradiol as related to estradiol receptor sites in breast tumor cytosol. Eur. J. Cancer Clin. Oncol., *18:* 333–337, 1982.
30. van Landeghem, A. A. J., Portman, J., and Nabauurs, M. Endogeneous concentration and subcellular distribution of estrogens in normal and malignant human breast tissue. Cancer Res., *45:* 2900–2906, 1985.
31. Blankenstein, M. A., Maitimu-Smeele, I., Donker, G. H., Daroszewski J., Milewicz, A., Thijssen, J. H. On the significance of in situ production of oestrogens in human breast cancer tissue. J. Steroid Biochem. Mol. Biol., *41:* 891–896, 1992.
32. Brodie, A. M., Lu, Q., Long, B. J., Fulton, A., Chen, T., Macpherson, N., DeJong, P. C., Blankenstein, M. A., Nortier, J. W., Slee, P. H., *et al.* Aromatase and Cox-2 expression in human breast cancers. J. Steroid Biochem. Mol. Biol., *79:* 41–47, 2001.
33. Lipton, A., Santen, R. J., Santen, S. J., Harvey, H. A., Peil, P. D., White-Hershey, D., Bartholomew, M. J., and Antle, C. E. Aromatase activity in primary and metastatic human breast cancer. Cancer (Phila.), *59:* 779–783, 1987.
34. Rebar, R. W., Morandini, I. C., Erickson, G. F., and Petze, J. E. The hormonal basis of reproductive defects in athymic mice: diminished gonadotropin concentration in prepubertal females. Endocrinology, *108:* 120–126, 1981.
35. Sutherland, R. L., Hall, R. E., and Taylor, I. W. Cell proliferation kinetics of MCF-7 human mammary carcinoma cells in culture and effects of tamoxifen on exponentially growing and plateau-phase cells. Cancer Res., *43:* 3998–4006, 1983.
36. Diel, P., Smolnikar, K., and Michana, H. The pure antiestrogen ZM 182,780 is more effective in the induction of apoptosis and down-regulation of BCL-2 than tamoxifen in MCF-7 cells. Breast Cancer Res. Treat., *58:* 87–97, 1999.
37. Long, B. J., Tilghman, S. L., Yue, W., Thiantanawat, A., Grigoryev, D. N., and Brodie, A. M. H. The steroidal antiestrogen ICI 182,780 is an inhibitor of cellular aromatase activity. J. Steroid Biochem. Mol. Biol., *67:* 293–304, 1998.
38. Huang, Y., Ray, S., Reed, J. C., Ibrado, A. M., Tang, C., Nawabi, A., and Bhalla, K. Estrogen increases intracellular p26Bcl-2 to p21Bax ratios and inhibits Taxol-induced apoptosis of human breast cancer MCF-7 cells. Breast Cancer Res. Treat., *42:* 73–81, 1997.
39. Zhang, G. J., Kimijima, I., Abe, R., Kanno, M., Katagata, N., Hara, K., Watanabe, T., and Tsuchiya, A. Correlation between the expression of apoptosis-related bcl-2 and p53 oncoproteins and the carcinogenesis and progression of breast carcinomas. Clin. Cancer Res., *3:* 2329–2336, 1997.
40. Perillo, B., Sasso, A., Abbondanza, C., and Palumbo, G. 17β-Estradiol inhibits apoptosis in MCF-7 cells, Inducing *bcl-2* expression via two estrogen-responsive elements present in the coding sequence. Mol. Cell. Biol., *20:* 2890–2901, 2000.
41. Zhang, G., Kimijima, I., Onda, M., Kanno, M., Sato, H., Watanabe, T., Tsuchiya, A., Abe, R., and Takenoshita, S. Tamoxifen-induced apoptosis in breast cancer cells related to down-regulation of bcl-2, but not bax and bcl-X_L, without alteration of p53 protein levels. Clin. Cancer Res., *5:* 2971–2977, 1999.
42. Hengartner, M. O. The biochemistry of apoptosis. Nature (Lond.), *407:* 770–776, 2000.
43. Susin, S. A., Lorenzo, H. K., Zamzami, N., Marzo, I. Brenner, C., Larochette, N., Prevost, M. C., Alzari, P. M., and Kroemer, G. Mitochondrial release of caspase-2 and -9 during the apoptotic process. J. Exp. Med., *189:* 381–394, 1999.
44. Li, P., Nijhawan, D., Budihardjo, I., Srinivasula, S. M., Ahmad, M., Alnemri, E. S., and Wang, X. Cytochrome *c* and dATP-dependent formation of Apaf-1/caspase-9 complex initiates an apoptotic protease cascade. Cell, *91:* 479–489, 1997.
45. Slee, E. A., Harte, M. T., Kluck, R. M., Wolf, B. B., Casiano, C. A., Newmeyer, D. D., Wang, H., Reed, J. C., Nicolson, D. W., Alnemri, E. S., Green, D. R., and Martin, S. J. Ordering the cytochrome *c*-initiated caspase cascade: hierarchical activation of caspase-2, -3, -6, -7, -8, and -10 in a caspase-9-dependent manner. J. Cell Biol., *144:* 281–292, 1999.
46. Cohen, G. M. Caspases: the executioners of apoptosis. Biochem. J., *326* (Pt. 1)*:* 1–16, 1997.
47. Fraser, A., and Evan, G. A license to kill. Cell, *85:* 781–784, 1996.
48. Srinivasula, S. M., Fernandes-Alnemri, T., Zangrilli, J., Robertson, N., Armstrong, R. C., Wang, L., Trapani, J. A., Tomaselli, K. J., Litwack, G., and Alnemri, E. S. The Ced-3/interleukin 1β converting enzyme-like homolog Mch6 and the lamin-cleaving enzyme Mch2α are substrates for the apoptotic mediator CPP32. J. Biol. Chem., *271:* 27099–27106, 1996.
49. Slee, E. A., Adrian, C., and Martin, S. J. Executioner caspase-3, -6, and -7 perform distinct, non-redundant roles during the demolition phase of apoptosis. J. Biol. Chem., *276:* 7320–7326, 2001.
50. Kuida, K., Zheng, T. S., Na, S., Kuan, C., Yang, D., Karasuyama, H., Rakic, P., and Flavell, R. A. Decreased apoptosis in the brain and premature lethality in CPP32-deficient mice. Nature (Lond.), *384:* 368–372, 1996.
51. Carroll, J. S., Prall, O. W. J., Musgrove, E. A., and Sutherland, R. L. A pure estrogen antagonist inhibit cyclin E-Cdk2 activity in MCF-7 breast cancer cells and induces accumulation of p130–E2F4 complexes characteristic of quiescence. J. Biol. Chem., *275:* 38221–38229, 2000.
52. Sionov, R. V., and Haupt, Y. The cellular response to p53: the decision between life and death. Oncogene, *18:* 6145–6157, 1999.
53. Ko, L. J., and Prives, C. p53: puzzle and paradigm. Gene Dev., *10:* 1054–1072, 1996.
54. Haldar, S., Negrini, M., Monne, M., Sabbioni, S., and Croce, C. M. Down-regulation of bcl-2 by p53 in breast cancer cells. Cancer Res., *54:* 2095–2097, 1994.
55. Dubik, D., and Shiu, R. P. C. Mechanism of estrogen activation of *c-myc* oncogen expression. Oncogene, *7:* 1587–1594, 1992.
56. Galaktionov, K., Chen, X., and Beach, D. Cdc25 cell-cycle phosphatase as a target of c-myc. Nature (Lond.), *382:* 511–517, 1996.
57. Yang, W., Shen, J., Wu, M., Arsura, M., FitzGerald, M., Suldan, Z., Kim, D. W., Hofmann, C. S., Pianetti, S., Romieu-Mourez, R., Freedman, L. P., and Sonenshein, G. E. Repression of transcription of the p27 (Kip1) cyclin-dependent kinase inhibitor gene by c-Myc. Oncogene, *20:* 1688–1702, 2001.
58. Yu, Q., Geng, Y., and Sicinski, P. Specific protection against breast cancers by cyclin D1 ablation. Nature (Lond.), *411:* 1017–1021, 2001.

Signaling Pathways of Apoptosis Activated by Aromatase Inhibitors and Antiestrogens

Apinya Thiantanawat, Brian J. Long and Angela M. Brodie

Cancer Res 2003;63:8037-8050.